Symbiosis
https://doi.org/10.1007/s13199-020-00680-1

Contrasting bacteriome of the hornwort *Leiosporoceros dussii* in two nearby sites with emphasis on the hornwort-cyanobacterial symbiosis

R. Bouchard[1,2] · G. Peñaloza-Bojacá[3] · S. Toupin[1,2] · Y. Guadalupe[4] · J. Gudiño[4] · N. Salazar Allen[4] · F. W. Li[5,6] · J. C. Villarreal A.[1,2,6]

Received: 1 March 2020 / Accepted: 23 April 2020

Abstract

Symbioses between plants and nitrogen-fixing cyanobacteria are benchmark biological systems to understand mutualism and patterns of coevolution. The diversity of cyanobacteria associated to non-vascular land plants is still being unraveled, with a huge gap in knowledge from tropical areas, especially in hornworts. We focus on the Neotropical hornwort *Leiosporoceros dussii*, which has a semi-permanent association with cyanobacteria. Unlike other hornworts, the peculiar *Nostoc* canals suggest cyanobiont specificity and selectivity. Here, we characterize the first hornwort bacteriome and focus on the endophytic cyanobacteria by describing its morphology, metagenomic diversity and phylogeny between two sampling sites in Panama. First, we use a metagenomic analyses (16S) from gametophytes from Río El Guayabo and Río Indio in Panama to identify the endophytic bacteria community of *L. dussii*. To provide more information on the cyanobacterial endophytes, we have extracted cyanobacterial endophytes to measure cell size variation and use the markers trnL and rbcLX to determine their phylogenetic relationships. Finally, we use stable isotope $\delta^{15}N$ to assess nitrogen flow in the plants. We find little diversity in *Leiosporoceros* bacteriome but observe significant community variations between sites. Results indicate a lack of cyanobacterial specificity of cyanobacteria associated to *Leiosporoceros*, with six unrelated clades of *Nostoc* forming a polyphyletic assemblage. Four clades are nested within bacteria collected as free-living taxa suggesting that typically non-symbiotic cyanobacteria can be associated with this hornwort. Finally, the little nitrogen fractioning of the plant suggests the role of the cyanobacterial symbionts in nitrogen fixation. This study provides the first hornwort bacteriome and is an important step in the characterization of tropical bryophyte symbioses.

Keywords Metagenomic · 16S · trnL · rbcLX · Stable isotope · Phylogenetic · Nitrogen · Bacteriome · Tropical bryophyte

R. Bouchard and G. Peñaloza-Bojacá contributed equally to this work.

Electronic supplementary material The online version of this article (https://doi.org/10.1007/s13199-020-00680-1) contains supplementary material, which is available to authorized users.

✉ J. C. Villarreal A.
juan-carlos.villarreal-aguilar@bio.ulaval.ca

[1] Institut de Biologie Integrative et des Systems, Quebec, Québec G1V 0A6, Canada

[2] Department of Biology, Université Laval, Quebec, Québec G1V 0A6, Canada

[3] Laboratório de Sistemática Vegetal, Departamento de Botânica, Instituto de Ciências Biológicas, Universidade Federal de Minas Gerais, Av. Antônio Carlos, 6627, Pampulha, Belo Horizonte, MG 31270-901, Brazil

[4] Smithsonian Tropical Research Institute, Panama City, Panama

[5] Boyce Thompson Institute, Ithaca, NY, USA

[6] Plant Biology Section, Cornell University, Ithaca, NY, USA

1 Introduction

Nitrogen is essential for plant growth, although the availability of reduced nitrogen in soil is often a limiting factor (Lodge et al. 1994; LeBauer and Treseder 2008). Diazotrophic bacteria use nitrogenase to convert atmospheric dinitrogen (N_2) to ammonia (NH_3) that can be absorbed by plants (Darnajoux et al. 2014; Nelson et al. 2019). Among diazotrophic bacteria, filamentous cyanobacteria are the prevalent N_2 fixers in aquatic ecosystems but also in many terrestrial environments (Lindo et al. 2013; Rousk et al. 2013; Arróniz-Crespo et al. 2014). Interestingly, a few land plants forming a polyphyletic assemblage have evolved to establish endophytic symbioses with cyanobacteria. These include one fern genus (*Azolla*, Salviniales), all cycads (Cycadophyta), one genus of

Published online: 30 May 2020

angiosperms (*Gunnera*, Gunnerales), two genera of one thalloid liverwort order (Blasiales, Marchantiophyta) and all (i.e., 220) species of hornworts (Costa et al. 2004; Adams and Duggan 2008).

Symbiosis with cyanobacteria of the genus *Nostoc* is a universal feature of hornwort gametophytes with all but one species (*Leiosporoceros dussii* (Steph.) Hässel) having minute globose colonies originally invaded by hormogonia through ventral pores (Renzaglia 1978; Meeks 2007). In most hornworts, the presence of multiple cyanobacterial colonies per gametophyte suggests a constant recruitment from available soil cyanobacteria, lack of selectivity and specificity. Until now, there had been only two studies that documented genetic diversity of cyanobionts from hornworts; these were limited to two temperate species: *Anthoceros fusiformis* Aust. ($n = 7$) using the *trnL* intron and *Phaeoceros laevis* (Michx.) Prosk. ($n = 19$) using DNA amplification fingerprinting (West and Adams 1997; Costa et al. 2001). While both studies count one to several cyanobiont genotypes per gametophyte thallus, the sampling was limited to a single species at a single site. Therefore, hornwort-cyanobiont specificity and spatial structure of other bacterial symbionts remain unexplored at a local and a global scale. In fact, there is not a single study on the bacteriome diversity of hornworts, with the assumption that only cyanobacteria colonized their gametophytes. We investigated the bacteriome, with emphasis on cyanobacteria, of the neotropical hornwort *Leiosporoceros dussii.*

Leiosporoceros dussii occupies a unique position in hornwort phylogeny, being sister to the rest of extant hornwort species (Villarreal and Renzaglia 2006). Furthermore, the development of the cyanobacterial colonies of *Leiosporoceros* contrasts with that in all other hornworts. In mature gametophytes, the *Nostoc* cyanobionts form long and branching strands that run parallel to the thallus main axis and grow in synchrony with the thallus, which grows all year round in a semi-permanent fashion (Villarreal and Renzaglia 2006). The emblematic ventral clefts, feature of all hornworts, are only produced at a sporeling stage and they cease developing after the plant gets infected. The absence of clefts in mature gametophytes precludes further cyanobacterial infections, suggesting that cyanobionts associated to *Leiosporoceros* could indeed have evolved specificity. This developmental constraint and its key phylogenetic position invite to first, test for specificity and second, to describe the bacterial diversity associated to this Neotropical plant. Therefore, we pose the question whether only cyanobacteria inhabit this emblematic hornwort and whether there is any spatial or phylogenetic structure in the symbionts.

In this study, we provided the first account of a hornwort bacteriome and illustrate the diversity of cyanobacteria associated to the Neotropical species, *L. dussii.* We focused on bacteriome diversity and selectivity associated to *Leiosporoceros* from two nearby sites in central Panama. We used a metagenomic approach (16S), morphology and sequence data to uncover the taxonomic breadth of the symbiotic strains targeting all bacteria (16S) and cyanobacteria (*trnL* intron and *rbcLX*). In addition, we used stable $\delta^{15}N$ isotope to address nitrogen cycling in the hornwort and whether the cyanobacteria associated to *Leiosporoceros* are fixing nitrogen for the host.

2 Materials and methods

2.1 Sampling for morphological and genotyping analyses

For morphological measurements, 20 collections from Río El Guayabo (5 male and 5 female plants) and Río Indio (5 male and 5 female plants) were used (Fig. 1). For each plant we described the cyanobiont by measuring the length and width of ten heterocysts and ten vegetative cells at 100X. All measurements were done with a light microscope model OLYMPUS: BX50 with the DP2-BSW OLYMPUS software. For the molecular analyses, gametophytes of *L. dussii* were sampled in Río Indio ($n = 19$) and in Río El Guayabo ($n = 13$; El Valle de Antón; Fig. 1a; Table 1) in 2017. Both sites are nearly three km apart and occur at an elevation of ~642 m. One collection from El Guayabo made in 2006 (JC12) was also included. In addition to these two sites, we have one accession from Palo Seco, comarca de Gnöbe Buglé ($n = 2$) and from Volcán Turrialba, Costa Rica (made in 2006). Within a locality, samples were taken 1 to 5 m apart to decrease the likelihood of collecting clonal plants. Thalli were kept in a plastic bag at 4 °C until DNA extraction. The thalli were then cleaned with sterile water to clean epiphytic cyanobacteria. To ensure sampling only endophytic cyanobacteria, the colonies were exposed by removing the epidermis with sterile razor blades. From these samples, 16 accessions (ten from El Guayabo and six from Río Indio) were used for further metagenomic work using 16S, see below. Accessions used in the study for DNA extraction are found in Table 1 and Table S4.

2.2 DNA extraction, metagenomic markers and cyanobacterial genes

16S metagenomics DNA was extracted using a E.Z.N.A. DNA (Omega, Bio-Tek, Norcross, US) extraction kit. The final elution volume was reduced to 30 μl. A two-step PCR was done to target the v3-v4 region of the 16S gene using an amplicon sequencing protocol developed at Laval University (Vincent et al. 2017). The locus-specific primers, BactV3-V4-F (341F) and BactV3-V4-R (805R), were selected for the first PCR from Klindworth et al. (2013), and were modified to include Illumina TruSeq

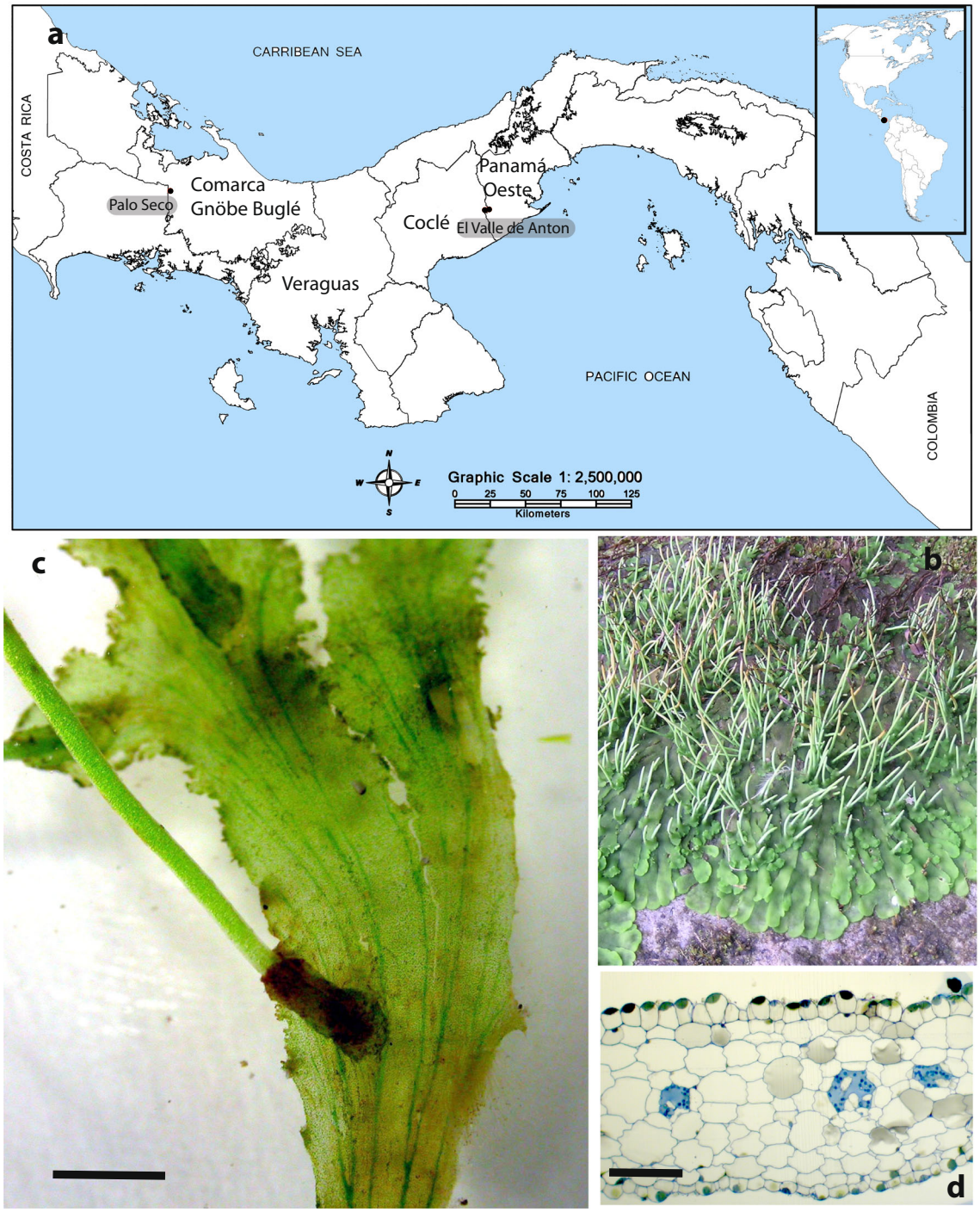

Fig. 1 **a** Geographical position of Panama on the American continent (inset, red dot). Map of collecting sites (red dots) in Panama, in the province of Coclé (Río El Guayabo and Río Indio) and in the comarca de Gnöbe Buglé (Palo Seco). **b** Colony of *Leiosporoceros dussii* growing on rock. Notice the strap-shaped thallus and the abundant sporophyte production. Plants on soil tend to grow more clonally. **c** Dichotomous strands of *Nostoc* parallel to the main axis of the thallus in a female plant with a single sporophyte. Unlike all other hornworts, the cyanobacteria occupy a large portion of the gametophyte, suggesting extensive interactions between partners. Bar 2 mm. **d** Transverse section of a young thallus with three central *Nostoc* canals. Light microscopy photo courtesy of Karen Renzaglia (Southern Illinois University, Carbondale). Bar = 100 μm

adaptors on their 5′ ends. PCR was conducted in a total volume of 25 μL that contained 1X Q5 buffer (NEB), 0.25 μM of each primer, 200 μM of each dNTPs, 1 U of Q5 High-Fidelity DNA polymerase (NEB) and 1 μL of template DNA. The second PCR introduced indexes and Illumina barcodes used in sequence library construction. The PCR protocols were respectively: PCR1: 98 °C for 2 min followed by 35 cycles of 98 °C for 10 s, 55 °C for

Table 1 Samples of *Leiosporoceros dussii i*n Río Indio and in Río El Guayabo

Voucher number	Collector	Country	Province, site	DNA #	trnL	rbcL-X
PA-17-1771	Villarreal, J.C.	Panama	Coclé	JC1012	MT347940	–
PA-17-1771	Villarreal, J.C.	Panama	Coclé	JC1013	MT347941	–
PA-17-1772	Villarreal, J.C.	Panama	Coclé	JC1014	MT347942	MT370453
PA-17-1772	Villarreal, J.C.	Panama	Coclé	JC1015	MT347954	–
PA-17-1765	Villarreal, J.C.	Panama	Gnöbe Buglé	JC1016	MT347939	MT370451
PA-17-1765	Villarreal, J.C.	Panama	Gnöbe Buglé	JC1017	–	MT370450
PA-17-1650 #8	Villarreal, J.C.	Panama	Río Indio	JC1018	MT347971	–
PA-17-1661 #19	Villarreal, J.C.	Panama	Río El Guayabo	JC1020	MT347947	MT370452
PA-17-1652 #10	Villarreal, J.C.	Panama	Río Indio	JC1021	MT347972	–
PA-17-1656 #14	Villarreal, J.C.	Panama	Río Indio	JC1022	MT347973	–
PA-17-1644 #2	Villarreal, J.C.	Panama	Río Indio	JC1023	–	MT370443
PA-17-1651 #9	Villarreal, J.C.	Panama	Río Indio	JC1024	MT347974	–
PA-17-1648 #6	Villarreal, J.C.	Panama	Río Indio	JC1025	–	MT370442
PA-17-1653 #11	Villarreal, J.C.	Panama	Río Indio	JC1026	MT347949	–
PA-17-1653 #11	Villarreal, J.C.	Panama	Río Indio	JC924	MT347948	–
PA-17-1647 #5	Villarreal, J.C.	Panama	Río Indio	JC925	MT347950	MT370449
PA-17-1652 #10	Villarreal, J.C.	Panama	Río Indio	JC934	MT347951	–
PA-17-1646 #4	Villarreal, J.C.	Panama	Río Indio	JC935	MT347952	MT370448
PA-17-1654 #15	Villarreal, J.C.	Panama	Río Indio	JC938	MT347975	MT370447
PA-17-1654 #12	Villarreal, J.C.	Panama	Río Indio	JC939	xMT347963	–
PA-17-1654 #12	Villarreal, J.C.	Panama	Río Indio	JC940	MT347964	–
PA-17-1649 #7	Villarreal, J.C.	Panama	Río Indio	JC941	MT347965	MT370446
PA-17-1649 #7	Villarreal, J.C.	Panama	Río Indio	JC942	MT347966	MT370445
PA-17-1643 #1	Villarreal, J.C.	Panama	Río Indio	JC943	MT347967	MT370444
PA-17-1643 #1	Villarreal, J.C.	Panama	Río Indio	JC944	MT347968	–
PA-17-1664 #22	Villarreal, J.C.	Panama	Río El Guayabo	JC945	MT347957	MT370464
PA-17-1664 #22	Villarreal, J.C.	Panama	Río El Guayabo	JC946		MT370463
PA-17-1645 #3	Villarreal, J.C.	Panama	Río Indio	JC948	MT347953	–
PA-17-1654 #12	Villarreal, J.C.	Panama	Río Indio	JC958	MT347969	–
PA-17-1655 #13	Villarreal, J.C.	Panama	Río Indio	JC959	MT347970	–
PA-17-1663 #21	Villarreal, J.C.	Panama	Río El Guayabo	JC960	MT347955	MT370462
PA-17-1664 #22	Villarreal, J.C.	Panama	Río El Guayabo	JC961	MT347956	MT370461
PA-17-1667 #25	Villarreal, J.C.	Panama	Río El Guayabo	JC962	MT347943	MT370460
PA-17-1667 #25	Villarreal, J.C.	Panama	Río El Guayabo	JC963	MT347944	MT370459
PA-17-1659 #17	Villarreal, J.C.	Panama	Río El Guayabo	JC964	MT347958	MT370458
PA-17-1659 #17	Villarreal, J.C.	Panama	Río El Guayabo	JC965	MT347959	MT370457
PA-17-1660 #18	Villarreal, J.C.	Panama	Río El Guayabo	JC966	MT347960	MT370456
PA-17-1660 #18	Villarreal, J.C.	Panama	Río El Guayabo	JC967	MT347961	–
PA-17-1661 #19	Villarreal, J.C.	Panama	Río El Guayabo	JC968	MT347962	MT370455
PA-17-1662 #20	Villarreal, J.C.	Panama	Río El Guayabo	JC969	MT347945	–
PA-17-1662 #20	Villarreal, J.C.	Panama	Río El Guayabo	JC970	MT347946	MT370454
PA-2006-854A (2006)	Villarreal, J.C. & E.O. Rodríguez	Panama	Río El Guayabo	JC12	–	MT370465
CR-2006-JC882 (2006)	Villarreal, J.C. et al.	Costa Rica	Volcán Turrialba	JC38	–	MT370466

30 s and 72 °C for 30 s with a final extension of 72 °C for 2 min; PCR2: 98 °C for 2 min followed by 12 cycles of 98 °C for 10 s, 60 °C for 30 s and 72 °C for 30 s with a final extension of 72 °C for 2 min. PCR reactions were purified using the Axygen PCR cleanup kit (Axygen). Quality of the purified PCR products was checked on a 1% agarose gel and then quantified spectrophotometrically with the Nanodrop 1000 (Thermo Fisher Scientific, Waltham). The libraries

were pooled using an equimolar ratio, quantified and sequenced on an Illumina MiSeq 300 bp paired-end run (600 cycle, v3 kit).

2.3 Diversity metrics and statistical analysis

All fastq sequences files were imported to R (R Core Team 2017) using RStudio V.3.6.0 (RStudio Team 2015) and the Bioconductor package V.3.9.0 (Callahan et al. 2017). The data was processed through the DADA2 pipe V.1.12.1 (Callahan et al. 2016a). DADA2 analysis was executed as described in https://benjjneb.github.io/dada2/tutorial.html, varying the parameters of filtering and trimming depending on the quality of the readings (trimLeft = (15,0), truncLen = c (250,210)) and inferred error rates. Subsequently, the final paired reads were merged, the chimeras were eliminated, and taxonomy assigned with the reference database *'silva_nr_v132_train_set'* for 16S rRNA using the naive Bayesian classifier method implemented in DADA2 (Callahan et al. 2016a). Amplicon sequence variants (ASVs) that were taxonomically assigned to mitochondria or chloroplast were removed as well as those ASVs with less than 10 reads.

2.4 Richness and diversity index nonparametric Chao1

The Chao1 index estimates the expected number of ASVs per sample in the two locations (El Guayabo and Río Indio) based on the number of low abundance ASVs, allowing to recognize the possible gaps between observed ASVs and a theoretical maximum (Gotelli and Colwell 2001; Hughes et al. 2001). The Shannon's index (considers equal weight among rare and abundant species) and Simpson's diversity index (assesses the probability that two sampled individuals belong to different ASVs) for the *Leiosporoceros* community were calculated using the phyloseq package (McMurdie and Holmes 2013). To test whether the observed number of ASVs differed significantly between the two sites, we performed a non-parametric test, the Mann-Whitney U test (Mann-Whitney) using the vegan package V2.5–5; Oksanen et al. 2019). The normalized ASVs abundance data were used for visualization of ASVs relative abundances and beta-diversity analysis. Relative phylum-level abundances and beta-diversity of bacterial communities were shown in *stacked barplot* with ggplot2 (Wickham and Chang 2009). Ordinations including principal coordinates analysis (PCoA) with Bray–Curtis and non-metric multidimensional scaling (NMDS), were generated using non-rarefied log transformed or rank abundance data (Callahan et al. 2016b), and generated using the *ordinate* and *plot_ordination* functions from phyloseq. We also tested for significant differences in the beta-diversity of the communities using *ANOSIM* from the vegan package (Dixon 2003) with 1000 permutations.

2.5 Cyanobacterial phylogenetic diversity: trnL and rbcLX sanger-sequencing and analyses

Two molecular markers, *trn*L and the *rbc*LX operon were amplified by PCR using the previously published primers (Wright et al. 2001; Rudi et al. 1998). Each 25 μl PCR reaction included: 25 μg BSA, 0,626 U *Taq* DNA polymerase (Qiagen), 1.5 mM $MgCl_2$, dNTPs (0.2 mM each), primers (0,5 μM forward and reverse) and 1X PCR buffer. The thermocycler temperature profile for both *rbc*LX and of *trn*L was: a 95 °C denaturation temperature for 5 min, followed by 35 cycles at 95 °C for 45 s, 52 °C for 45 s and 72 °C for 1:30 min, with a final extension of 72 °C for 10 min for *rbc*LX and of 7 min for *trn*L.

The chromatograms were analysed using Geneious 9.0.5 (Biomatters Limited, Auckland). The *trnL* sequences were aligned using the intron secondary structure. To establish diversity and phylogenetic position of *L. dussii*'s cyanobionts, the *rbcLX* sequences generated by O'Brien et al. (2005) and Magain et al. (2016) were added to the alignment. We analyzed only the genes *rbcL* and *rbcX*, removing the spacers, of 599 sequences of cyanobacteria associated to lichens, plants (*Gunnera*, cycads, bryophytes) and cyanobacteria collected as "free-living". Duplicates were removed and the final matrix had 485 accessions (Table S4). Branch support was assessed by maximum-likelihood (ML) bootstrapping. The ML analysis was conducted using RAxML version 8.0 (Stamatakis 2014), using the default model of evolution. Statistical support was evaluated via 500 ML bootstrap pseudoreplicates.

For Sanger-sequencing analyses, no cloning was performed. Villarreal and Renzaglia (2006) have shown that the dichotomously branched *Nostoc* strands is the result of a single cyanobacterial invasion. After the initial infection at the sporeling stage, the strands elongate and branch in synchrony with apical growth. In our sampling design, each cyanobiont was isolated from a single strand and tissue around it. Since only one putative *Nostoc* species is isolated for each extraction, we use standard *rbcLX* and *trnL* Sanger-sequencing to evaluate phylogenetic relationships. Additionally, most studies of symbiotic cyanobateria (in lichens) have found a dominant strain within each cyanobacterial colony (Costa et al. 2001; Fedrowitz et al. 2011; Pardo-De la Hoz et al. 2018; Lavoie et al. 2020).

2.6 Isotope analyses

We collected 9 samples, five gametophytes from Río Indio (with *Nostoc*) and four from Río Guayabo. We removed the soil under individual gametophytes to explore the relationship between $\delta^{15}N$ values in the gametophyte and available soil N. All gametophyte tissue was cleaned of damaged tissue before being dried at 60 °C for 48 h, and ground to a fine powder. The

soil was equally dried at 60 °C for 48 h. The total weight used was 2 mg and 10 mg (soil). We used Aspartic Acid with 10.52% of N, to calibrate the sequence and also used internal standards. We outsourced the isotopic analyses to the Smithsonian Tropical Research Institute's Stable Isotope Laboratory. Stable isotope abundances are reported as: δ15N = (Rsample/Rstandard $^{-1}$) × 1000, where R = ^{15}N:^{14}N ratio of the sample or standard. Based on three internal standards the run error rates were 0.05% and analytical precision for the samples analyzed in duplicates. The significance of the difference in mean values between plant and soil samples was assessed with a Mann-Whitney U test (non-parametric test was used because of the small size of the dataset and its distribution) in R.

3 Results

3.1 Morphological characterization of the cyanobionts

All collections of *Leiosporoceros*, from all collecting sites, have the *Nostoc* canals regardless of the size of the gametophyte (Figs. 1b-d, 4b, Fig. S3). The endophytic cyanobacteria have a general appearance of the genus *Nostoc* and *Anabaena*. The vegetative cells and heterocysts from Río Indio populations tend to have a smaller size and more rounded cells (Fig. S2). Cyanobacteria from Río Guayabo tend to vary from spherical to oval and the coloration is bluish green to yellowish green in color. The frequency of heterocysts seem to be high (25–35%) especially in older sections of the thalli (data not shown) as previously suggested for the species (Villarreal and Renzaglia 2006, Fig. S3).

3.2 *Leiosporoceros dussii* bacteriome richness and diversity

We analyzed the *L. dussii* associated bacterial bacteriome using 16S rRNA amplicons generated a total of 856,193 raw paired-end reads. After filtering there were 498,944 combined reads. Subsequently, chimera sequences were removed from the dataset, forming 328,133 reads (Table S1). In total, we found 1214 ASVs among the 16 samples (Table S2).

The non-parametric Chao1 index estimated that our ASVs were close to the theoretical optimum. Coverage was greater than 97% in both locations and for most samples (Table 2). The Shannon index (H′) indicated that the samples of *L. dussii* were diverse (H′ > 3.02). For Río Indio, the JC0940 sample presented the highest values (H' = 3.89), unlike the JC0925 sample with the lowest H′ (2.76). El Guayabo presented an H′ between 2.03 to 3.10 in seven of the ten samples. Samples JC0961, JC0966 and JC0968 showed a substantial low diversity with an H 'of 1.54, 1.88 and 1.37 respectively. The Simpson diversity index (D) from samples of Río Indio were of D > 0.88, except for JC0925 (D = 0.76). In El Guayabo, the highest values were D = 0.68–0.88 (Fig. 2a). There was a significant difference of abundance of ASVs for both the Shannon and Simpson diversity indices (p value = 0.0017 and p value = 0.011, respectively).

The ASVs were classified into 10 Phyla, 15 Classes, 48 Orders, 64 Families and 82 Genera. The phyla Proteobacteria (52.38%), Cyanobacteria (34.28%), Gemmatimonadetes (5.50%) and Acidobacteria (3.78%) had the highest relative abundance in the bacteriome (Fig. 2b, Tables 3, S3), unlike Verrucomicrobia, Chloroflexi and WPS-2 (<1%; Table S3). The most abundant families in Proteobacteria were Sphingomonadaceae (38.47%), Rhizobiaceae (28.11%) and Caulobacteraceae (12.93%; Fig. S1A). Regarding Cyanobacteria, the most abundant family was Nostocaceae (99.57%) in both areas, with a higher record in El Guayabo (92%) than in Río Indio (7.5%) (Fig. S1C; Table S2). The most representative genera in the *L. dussii* bacteriome for Proteobacteria were *Sphingomonas* (43.71%), *Allorhizobium-Neorhizobium-Pararhizobium-Rhizobium* (29.22%) and *Caulobacter* (15.31%), the latter being found mainly for Río Indio (15.26%; Fig. S1B). For Cyanobacteria, the *Nostoc* PCC-7524 (44.82%), *Nostoc* PCC-7107 (28.14%) and *Desmonostoc* PCC-7422 (19.21%) genera were predominant (Fig. S1D; Table S3). We additionally found the cyanobacterial genus *Gloeobacter*. Ordination analyzes (PCoA and NMDS) showed similar results with distinct grouping for each collection site (Fig. 3). In addition, the ANOSIM test was significative when comparing the beta-diversity of the communities (R: 0.3261 Significance: 0.00899)

3.3 Phylogenetic analyses

DNA from 28 specimens of *L. dussii* was extracted and used to generate 37 *trnL* sequences representing 11 different genotypes. Most sequences are highly similar, with polymorphism restricted to the P6 loop. Most cyanobacteria associated with *L. dussii* presented a class 2 pattern the P6b loop level, with the remainder (i.e., nine) showing a class 1 pattern. A single intron genotype is shared between Río Indio and El Guayabo, and another between Río Indio and Palo Seco (Fig. 4c; Fig. S4**)**.

A total of 25 sequences of *rbcLX* were amplified from 25 specimens of *L. dussii.* The ML phylogenetic analyses recovered that cyanobacteria associated with *L. dussii* occurred in six clades (Fig. 4a**)**. Two clades comprising cyanobacteria from Río Indio, Palo Seco and one sample from Costa Rica are regrouped in the *Nostoc II* clade (previously defined by O'Brien et al. 2005 in their Fig. 1a). Accessions from El Guayabo compose a polyphyletic assemblage with four distinct clades. Five cyanobionts from El Guayabo included a deletion of three amino acids at the 3′ end of *rbcLX* and ended with a TGA (versus a TAG) codon stop.

Table 2 Alpha diversity metrics for the samples of *Leiosporoceros dussii*

Area	Sample name	Observed	Chao1	Shannon	Simpson	InvSimpson
Río Indio	JC0925.S76	153	154	2.76	0.76	4.17
Río Indio	JC0935.S77	191	204	3.52	0.91	11.23
Río Indio	JC0940.S78	143	147	3.89	0.96	26.76
Río Indio	JC0943.S79	98	98	3.02	0.88	8.39
Río Indio	JC0944.S80	145	148	3.39	0.91	11.69
Río Indio	JC0948.S82	146	149	3.36	0.92	12.38
Río el Guayabo	JC0946.S81	76	78	2.78	0.88	8.65
Río el Guayabo	JC0961.S83	54	54	1.54	0.51	2.03
Río el Guayabo	JC0963.S84	85	87	2.03	0.79	4.67
Río el Guayabo	JC0964.S85	34	36	2.01	0.74	3.90
Río el Guayabo	JC0966.S86	68	68	1.88	0.59	2.44
Río el Guayabo	JC0967.S87	86	86	3.10	0.88	8.50
Río el Guayabo	JC0968.S88	44	53	1.37	0.54	2.16
Río el Guayabo	JC0969.S89	104	104	2.57	0.76	4.18
Río el Guayabo	JC1013.S90	174	175	2.58	0.68	3.09
Río el Guayabo	JC1014.S91	124	125	2.53	0.79	4.74

3.4 Isotope data

$\delta^{15}N$ for gametophytes range between −1.83 - 0.22% with a mean value of −1.22 (+ − 1.16) and (1.09) 5.05–11.26 ‰ from the soil under the plant with mean values of 7.71% (+ − 2.85; Fig. 5). A non-parametric test found the difference between the two sample types to be significant (p value 6.804×10^{-6}).

4 Discussion

The microbiome (fungi, viruses and bacteria) may have played a key role in early land plant colonization by facilitating nutrient uptake to the first land plants (Remy et al. 1994). Genomic evidence suggests that the streptophyte ancestor had already the capabilities for forming symbioses (Knack et al. 2015). In extant species, the microbiome still plays a crucial role in plant growth, fitness and survival. In contrast to tracheophytes, we are just starting to uncover the diversity of microbes associated to bryophytes. Most studies have been conducted on model species (*Marchantia spp.;* Alcaraz et al. 2018; Nelson and Shaw 2019; Nelson et al. 2018), boreal mosses (e.g. *Pleurozium schreberi*; DeLuca et al. 2002, 2007; Gentili et al. 2005), and liverworts (e.g. *Blasia*) and hornworts with endophytic cyanobacteria (Costa et al. 2001; Adams 2002). As in vascular plants, there is growing evidence of the crucial role of microbes in providing key elements such as phosphorous and nitrogen (Brookes et al. 1982; Barrow et al. 2008).

The best bryophyte-bacteria system studied to date is the association between cyanobacteria and hornworts and Blasiales, in which the cyanobacteria transferred fixed nitrogen (as ammonium) to the host plant (Adams 2002; Wong and Meeks 2002; Renzaglia et al. 2007). Despite the spectacular knowledge on the morphology, physiology, and genomics of the interaction, there is very little know about the diversity of

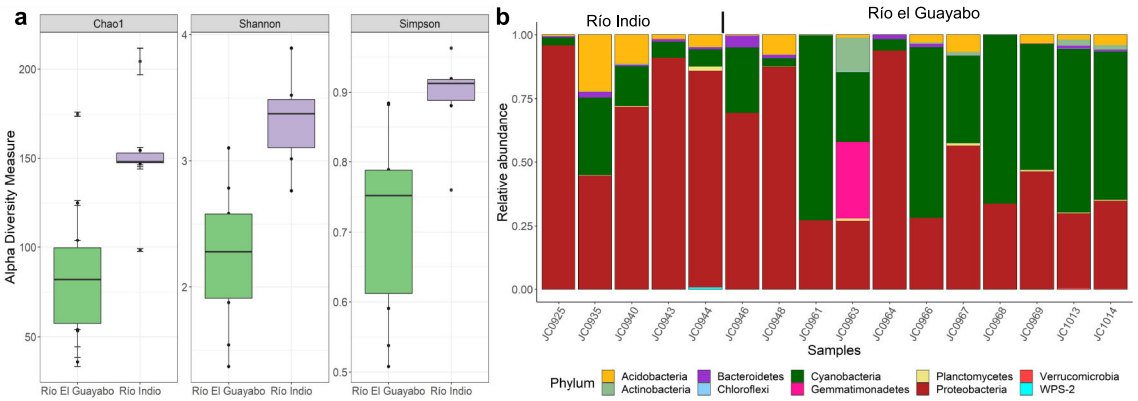

Fig. 2 Bacteriome diversity of the hornwort *Leiosporoceros dussii.* **a** Alpha diversity indices. **b** Relative abundance by taxa for each sample

Table 3 Main taxa present in the bacteriome of *Leiosporoceros dussii*

Site	Phylum	Abundance (reads)	%	Site	Phylum	Abundance	%	Phylum	Abundance	%
Río el Guayabo	Cyanobacteria	35,695	30.67	Río Indio	Proteobacteria	34,192	29.37	Proteobacteria	60,965	52.38
Río el Guayabo	Proteobacteria	26,773	23.00	Río Indio	Cyanobacteria	4204	3.61	Cyanobacteria	39,899	34.28
Río el Guayabo	Gemmatimonadetes	6394	5.49	Río Indio	Acidobacteria	3077	2.64	Gemmatimonadetes	6397	5.50
Río el Guayabo	Actinobacteria	3227	2.77	Río Indio	Bacteroidetes	438	0.38	Acidobacteria	4402	3.78
Río el Guayabo	Acidobacteria	1325	1.14	Río Indio	Planctomycetes	138	0.12	Actinobacteria	3275	2.81
Río el Guayabo	Bacteroidetes	426	0.37	Río Indio	Actinobacteria	48	0.04	Bacteroidetes	864	0.74
Río el Guayabo	Planctomycetes	308	0.26	Río Indio	WPS-2	46	0.04	Planctomycetes	446	0.38
Río el Guayabo	Chloroflexi	49	0.04	Río Indio	Verrucomicrobia	10	0.01	Verrucomicrobia	54	0.05
Río el Guayabo	Verrucomicrobia	44	0.04	Río Indio	Gemmatimonadetes	3	0.003	Chloroflexi	49	0.04
Río el Guayabo	WPS-2	3	0.003	Río Indio	Chloroflexi	0	0.000	WPS-2	49	0.04
Río el Guayabo		74,244	63.78	Río Indio		42,156	36.22	Total general	116,400	100.00
Site	**Family**	**Abundance**	**%**	**Site**	**Family**	**Abundance**	**%**	**Family**	**Abundance**	**%**
Río el Guayabo	Rhizobiaceae	10,281	18.62	Río Indio	Sphingomonadaceae	14,498	26.25	Sphingomonadaceae	21,245	38.47
Río el Guayabo	Sphingomonadaceae	6747	12.22	Río Indio	Caulobacteraceae	6800	12.31	Rhizobiaceae	15,522	28.11
Río el Guayabo	Pseudomonadaceae	1614	2.92	Río Indio	Rhizobiaceae	5241	9.49	Caulobacteraceae	7141	12.93
Río el Guayabo	Xanthobacteraceae	1195	2.16	Río Indio	Burkholderiaceae	2079	3.76	Burkholderiaceae	2415	4.37
Río el Guayabo	Beijerinckiaceae	946	1.71	Río Indio	Rhodanobacteraceae	547	0.99	Pseudomonadaceae	1719	3.11
Río el Guayabo	Acetobacteraceae	823	1.49	Río Indio	Beijerinckiaceae	399	0.72	Xanthobacteraceae	1354	2.45
Río el Guayabo	Hyphomicrobiaceae	381	0.69	Río Indio	Acetobacteraceae	283	0.51	Beijerinckiaceae	1345	2.44
Río el Guayabo	Caulobacteraceae	341	0.62	Río Indio	Elsteraceae	258	0.47	Acetobacteraceae	1106	2.00
Río el Guayabo	Burkholderiaceae	336	0.61	Río Indio	Xanthomonadaceae	173	0.31	Rhodanobacteraceae	881	1.60
Río el Guayabo	Rhodanobacteraceae	334	0.60	Río Indio	Xanthobacteraceae	159	0.29	Elsteraceae	534	0.97
Río el Guayabo		24,085	43.61	Río Indio		31,138	56.39	Total general	55,223	100.00
Area	**Genus**	**Abundance**	**%**	**Site**	**Genus**	**Abundance**	**%**	**Genus**	**Abundance**	**%**
Río el Guayabo	*Allorhizobium-Neorhizobium-Pararhizobium-Rhizobium*	7859	18.27	Río Indio	*Sphingomonas*	12,249	28.48	*Sphingomonas*	18,801	43.71
Río el Guayabo	*Sphingomonas*	6552	15.23	Río Indio	*Caulobacter*	6563	15.26	*Allorhizobium-Neorhizobium-Pararhizobium-Rhizobium*	12,570	29.22
Río el Guayabo	*Bradyrhizobium*	781	1.82	Río Indio	*Allorhizobium-Neorhizobium-Pararhizobium-Rhizobium*	4711	10.95	*Caulobacter*	6585	15.31
Río el Guayabo	*Mesorhizobium*	619	1.44	Río Indio	*Sphingobium*	699	1.63	*Bradyrhizobium*	812	1.89
Río el Guayabo	*Hyphomicrobium*	381	0.89	Río Indio	*Labrys*	147	0.34	*Sphingobium*	711	1.65
Río el Guayabo	*Methylobacterium*	227	0.53	Río Indio	*Rudaea*	138	0.32	*Mesorhizobium*	625	1.45
Río el Guayabo	*Labrys*	222	0.52	Río Indio	*Bosea*	132	0.31	*Hyphomicrobium*	451	1.05
Río el Guayabo	*Roseiarcus*	147	0.34	Río Indio	*Novosphingobium*	103	0.24	*Labrys*	369	0.86
Río el Guayabo	*Methylorosula*	130	0.30	Río Indio	*Tardiphaga*	83	0.19	*Methylobacterium*	306	0.71
Río el Guayabo	*Bosea*	91	0.21	Río Indio	*Methylobacterium*	79	0.18	*Bosea*	223	0.52

Table 3 (continued)

Río el Guayabo	*Acidisoma*	89	0.21	Río Indio	*Hyphomicrobium*	70	0.16	*Roseiarcus*	176	0.41
Río el Guayabo		17,693	41.13	Río Indio		25,322	58.87	Total general	43,015	100.00

The taxonomic groups are filtered by the ten most abundant taxa by site (Río El Guayabo and Río Indio). Family and genera corresponding to the Phylum Proteobacteria are shown on the table. Values in bold, represent the total abundance in the bacteriome

bacteria associated to hornworts. In this study, we provided the first account of a hornwort bacteriome and illustrate the diversity of cyanobacteria associated to the Neotropical species, *L. dussii*. The isotopic data confirm the little nitrogen fractioning of the cyanobacteria with mean values of −1.22 (+ − 1.16), typical of plants relying in nitrogen fixation (such as legume nodules).

4.1 Bacterial diversity

Among the few studies regarding the diversity of bacteria associated to mosses and liverworts, a common theme is the large diversity associated to wild populations of the species, the presence of a specific core microbiome, and a site-specific effect (Knack et al. 2015; Alcaraz et al. 2018; Nelson and Shaw 2019). Our study has two main findings regarding the overall hornwort bacteriome: 1) there is very little diversity of bacteria in *L. dussii*. For example, the wild plants of *Marchantia* spp. have abundant bacteria taxa (6000–10,000 OTUs vs 1214 ASVs in *Leiosporoceros*); 2) the bacteriome seems to be defined by site.

One explanation of such reduced diversity in niche competition. The large cyanobacterial channels inside of each plant (Villarreal and Renzaglia 2006), suggest a reduced niche for other bacterial taxa. The canals can make from 1/5 to half of the hornwort gametophytes, it is possible that there is inhibition of other bacteria. A similar level of competition has been suggested in the myco- and bacteriome of the coralloid roots of one species of the genus *Cycas* (Zheng et al. 2018). A similar specialized bacteriome has been also found in the epiphytic gymnosperm, *Zamia pseudoparasitica* (Bell-Doyon et al. 2020). In the cycads, the space or area occupied by the cyanobacteria covers most of the inner portion of the root and a similar situation occurs in the gametophyte of *Leiosporoceros*. In addition, hornworts with large *Nostoc* colonies, including *Leiosporoceros,* have been shown to be devoid of fungal endophytes (Desiró et al. 2013).

The bacteriome (including the cyanobacterial diversity) of *Leiosporoceros dussii* differs in each site, even if they are only 3 km apart. The reason of such disparity could be the soil type. The soil from El Guayabo is a white volcanic soil. The soil from Río Indio has a combination of volcanic soil and clay and slightly higher pH (up to 7.43 vs >7.0 in El Guayabo). The most common phyla found among our samples are Cyanobacteria, including the genus *Nostoc* sensu lato and *Gloeobacter*, the sister to all cyanobacterial taxa (Schirrmeister et al. 2013), and Proteobacteria. Among the Proteobacteria, Sphingomonadaceae, Rhizobiaceae *and* Caulobacteraceae are the most abundant among the samples mirroring the findings in many terrestrial lichens (Sierra et al. 2020). Caulobacteraceae and Sphingomonadaceae have been related to a number of lichen metabolic (e.g nitrogen, sulfur and iron metabolism) and stress response (Cernava et al. 2017). Caulobacteroaceae play a critical role in producing specialized metabolites linked to the interaction between cycad species and microbes (Gutiérrez-García et al. 2019). Despite the site-specific differences, both sites show a substantial diversity of Proteobacteria, especially those related to the diazotrophic Rhizobiales (Alcaraz et al. 2018). It is plausible that such bacteria contribute to the fixed nitrogen to the hornwort. The phyla with the lowest representation were Verrucomicrobia and WPS-2 (among others). The WPS-2 bacteria have been reported in boreal mosses and are anoxygenic phototrophs capable of carbon fixation (Holland-Moritz et al. 2018). Recent metagenomic analyses show that the phylum is mostly present in temperate, boreal and polar environments (Ward et al. 2019), but probably widespread in tropical settings as it was found in the coralloid roots of a Panamanian *Zamia* (Bell-Doyon et al. 2020).

4.1.1 Genotypic diversity using the trnL intron and lack of specificity or selectivity

Genetic diversity of *trnL* genotypes in *L. dussii* is elevated within each sampling site (Fig. 4c), in comparison to previous studies (Costa et al. 2001). We found no evidence of vertical transmission of the cyanobiont in *L. dussii* since no genotype is overrepresented in each population and allelic composition

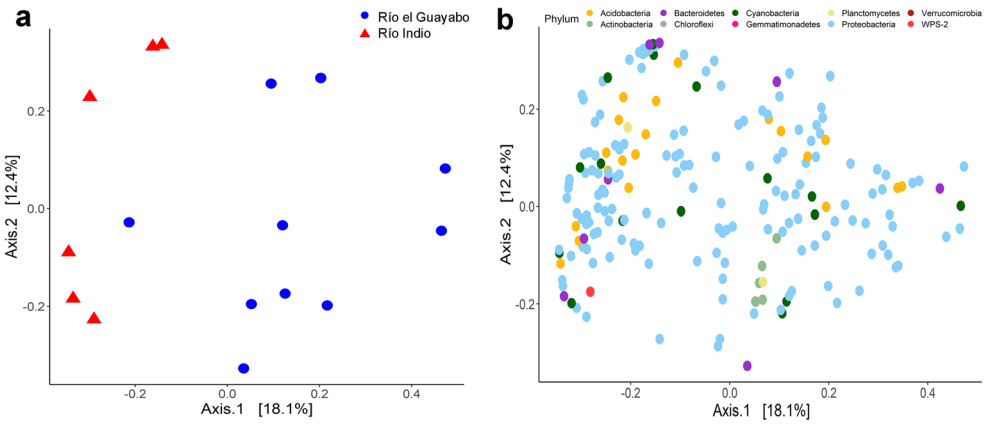

Fig. 3 Bacteriome diversity of the hornwort *Leiosporoceros dussii*. Ordination analysis based on Bray-Curtis distance. **a** Principle coordinates analysis (PCoA) by site. **b** PCoA analysis by phylum

of the *trnL* locus is almost completely different between Río Indio and El Guayabo, despite their close proximity (~ 3 km). However, we should interpret these results with caution since sampling is limited to two (three) sites and only two loci were used to examine genetic diversity.

Rikkinen and Virtanen (2008) found that the most dominant *Nostoc trnL* genotype from the liverwort *Cavicularia densa* (Blasiales) in Japan (Pr 10;Rikkinen and Virtanen 2008) occurred also in *Blasia pusilla* in central Finland. Similarly, O'Brien et al. (2005) found that a haplotype of a *Nostoc* associated to *Peltigera aphthosa* from Europe is likewise found in specimens of *Peltigera membranacea* from North America and Asia. Our results and these examples clearly indicate a considerable level of idiosyncratic spatial discontinuity in *Nostoc* symbioses in hornworts and other organisms.

4.1.2 Phylogenetic diversity using rbcLX and evolution of symbiosis

The major phylogenetic relationships inferred in this study are in broad agreement with other phylogenies of symbiotic cyanobacteria using *rbcLX* (O'Brien et al. 2005; Magain et al. 2016). We found striking phylogenetic differences between specimens from El Guayabo and Río Indio, despite their close proximity. Conversely, collections of *L. dussii*

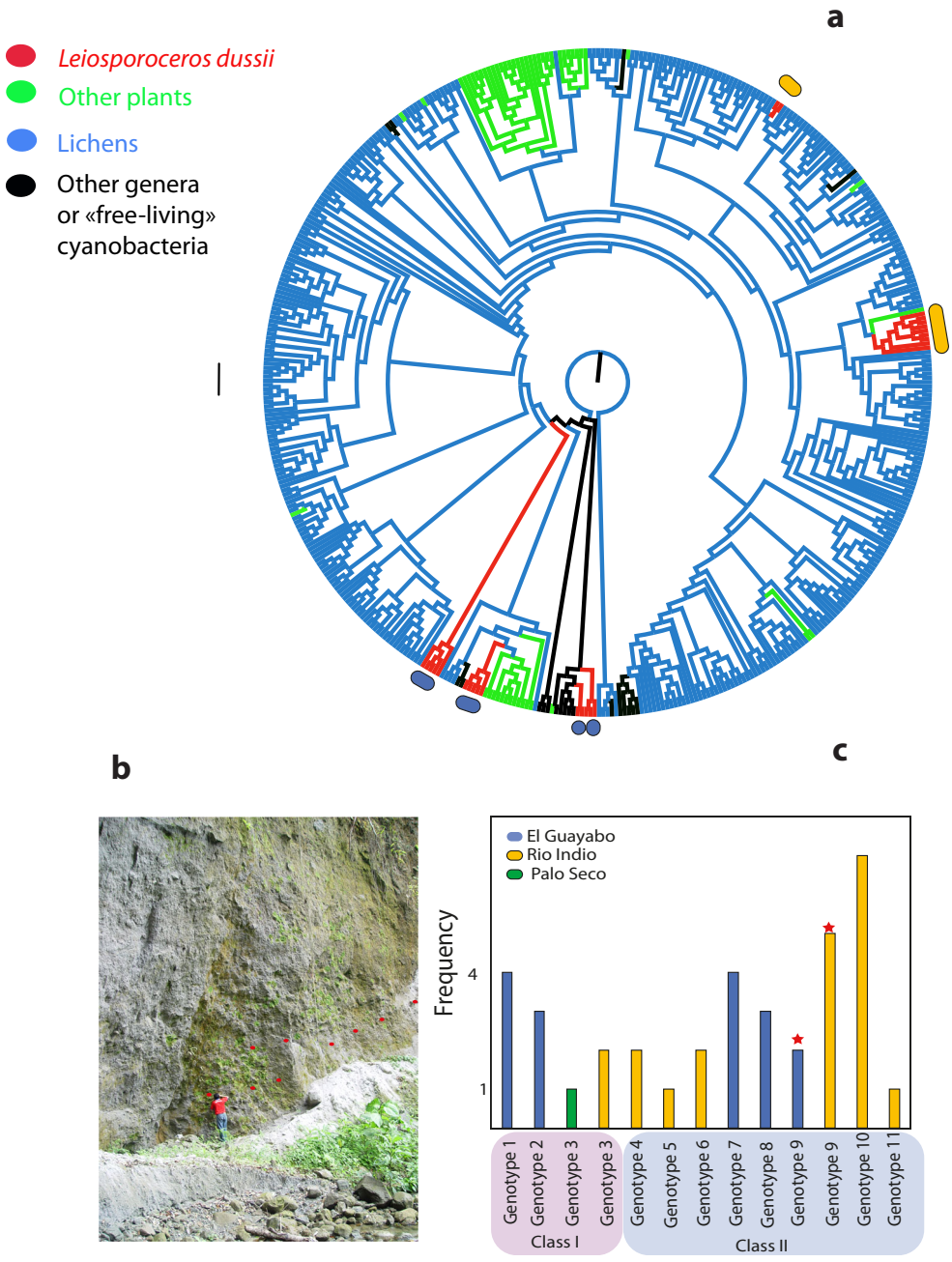

Fig. 4 **a** Phylogenetic relationships of cyanobacteria strains based on *rbcLX*. Bootstrap values are provided in the Figure S4. Clades in red represent *Leiosporoceros* accessions, those with a blue oval correspond to isolated *L. dussii* specimen strains from El Guayabo, while those with in yellow oval correspond to isolated specimen strains from Río Indio, Costa Rica and from Palo Seco. Thanks to Nicolas Magain (Duke University) for sharing his annotated dataset (Table S4). **b** A panoramic view of El Guayabo (Coclé) taken in 2003. The white soil is of volcanic origin. The collecting points on the wall are marked (red dots). The wall crumbles away periodically exposing new soil each time. **c** Genotype diversity in the P6b loop of *trnL*, cyanobacteria in association with *L. dussii*. Class1 – Pattern of class 1 heptanucleotide repetition: TDNGATT (Costa et al. 2002); Class2 – Pattern of class 2 heptanucleotide repetition: NNTGAGT (Costa et al. 2002) ($n = 37$). Shared genotypes between el Guayabo and Río Indio are red-starred

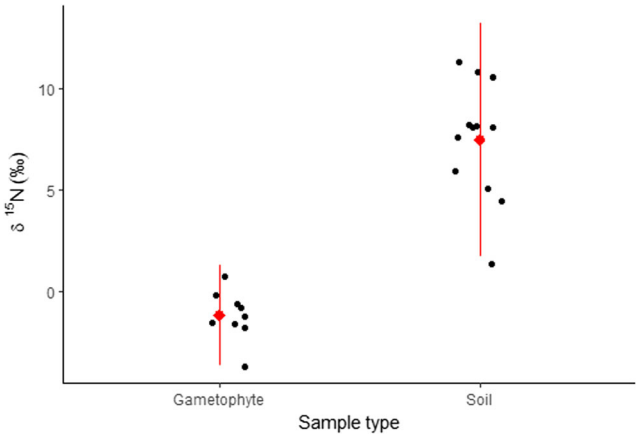

Fig. 5 Stable isotope (δ^{15}N in ‰) analysis results from *L. dussii* gametophytes and associated soil. The 95% interval is shown here by a red line crossing the mean, shown by a red dot

from Río Indio, Palo Seco and Costa Rica share phylogenetically close *Nostoc* strains, despite the larger geographic distance separating these populations, a common theme among lichens and thalloid liverworts (Costa et al. 2001; O'Brien et al. 2005; Rikkinen and Virtanen 2008).

The finding that two *Nostoc* strains isolated from Río Indio specimens were clustered with strains isolated from *Peltigera spp.* may be due to the sampling effort since most *rbcLX* phylogenies are biased toward lichen cyanobionts (see Joneson and O'Brien 2017). The sample JC12 was collected in 2006 (Table 1) and it's clustered within one clade of el Guayabo (JC970, 1020, 1014), suggesting that after 13 years of sampling similar strains may be associated with *L. dussii.*

Cyanobionts isolated from El Guayabo are distributed in four clades genetically different from *Nostoc* strains commonly found in symbioses. Two clades are nested within putatively free-living strains (Fig. 4). In contrast with earlier studies (Costa et al. 2001; Rikkinen and Virtanen 2008), our finding suggests that the phylotype diversity in *L. dussii* is mainly driven by local *Nostoc* strain pool rather than by species-level host specialization, mirroring the situation in some lichens (O'Brien et al. 2005, 2013).

The lack of selectivity and specificity can be due to the innovative morphological arrangement of the cyanobacterial filaments. The *Nostoc* filaments in *Leiosporoceros* are continuous along the length of the thallus (Fig. 1c), thus maintain continuity in addition to increasing surface contact for exchange between both partners (Villarreal and Renzaglia 2006). The innovative arrangement and development of *Nostoc* canals in *Leiosporoceros* could allow colonization by unusual heterocystous-forming cyanobacteria in a semi-permanent fashion. Finally, our isotope data confirm that *L. dussii* may be profiting the fixed nitrogen by the cyanobacteria as shown in other hornworts (Adams 2002; Wong and Meeks 2002) and the fractioned nitrogen in the soil under may be coming from leaching (or decomposition) of the thallus. The volcanic soil may be poor in nutrients and the hornwort-cyanobacterial symbiosis may contribute to the local budget. In addition, volcanic soil tends to be rich in vanadium (Schlesinger et al. 2017) favoring the unusual presence of cyanobacteria with an alternative nitrogenase in *Leiosporoceros* (Nelson et al. 2019).

5 Conclusion

Using a combination of metagenomic, sequence, morphological and isotopic approaches we have brought light into the symbiotic association between the hornwort *Leiosporoceros* and endophytic bacteria. This study provides the first account of a hornwort bacteriome. The most abundant phyla are Proteobacteria and Cyanobacteria. The little diversity of endophytic bacteria (only 1214 ASV in total) may be in response to the presence of cyanobacteria in competition with other bacteria. *Leiosporoceros* seems to receive fixed nitrogen from its partner using both Molybdenum- and Vanadium-type nitrogenases present in the cyanobacteria (Nelson et al. 2019) and potentially in Rhizobiales. We found a distinct bacteriome in the two sites and a phylogenetic diverse group of cyanobacteria associated to this hornwort. This study is an important step in the characterization of symbiosis in tropical bryophytes.

Authors' contributions RB and JCV conceived the study and performed the phylogenetic work and wrote the first version of the manuscript; GPB did the metagenomic analysis; ST performed the analysis of isotope data, YG did the morphological measurements, JG and NSA provided logistic support in the field and funding; FWL contributed with logistic support and funding; RB, GPB, NS, FWL, ST and JCV wrote and edited the manuscript.

Funding information *Établissement de nouveaux chercheurs universitaires* FRQNT- 206943 to JCVA.

Earl S. Tupper Fellowship 2015 to JCVA.

National Science Foundation Dimensions of Biodiversity grant (1831428) to F.-W.L.

Data availability The dataset generated and analysed during the current study is available from GenBank and DRYAD (https://doi.org/10.5061/dryad.sxksn030k).

Compliance with ethical standards

Conflicts of interest/competing interests Authors have no conflict of interest.

References

Adams DG (2002) Cyanobacteria in Symbiosis with hornworts and liverworts. In: Rai AN, Bergman B, Rasmussen U (eds) Cyanobacteria in Symbiosis. Springer, Dordrecht, pp 117–135. https://doi.org/10.1007/0-306-48005-0_7

Adams DG, Duggan PS (2008) Cyanobacteria-bryophyte symbioses. J Exp Bot 59:1047–1058. https://doi.org/10.1093/jxb/ern005

Alcaraz LD, Peimbert M, Barajas HR, Dorantes-Acosta AE, Bowman JL, Arteaga-Vázquez MA (2018) *Marchantia* liverworts as a proxy to plants' basal microbiomes. Sci Rep 8:1–12. https://doi.org/10.1038/s41598-018-31168-0

Arróniz-Crespo M, Pérez-Ortega S, De Los RA et al (2014) Bryophyte-cyanobacteria associations during primary succession in recently deglaciated areas of Tierra del Fuego (Chile). PLoS One 9:15–17. https://doi.org/10.1371/journal.pone.0096081

Barrow JR, Lucero ME, Reyes-Vera I, Havstad KM (2008) Do symbiotic microbes have a role in regulating plant performance and response to stress? Commun Integr Biol 1:69–73. https://doi.org/10.4161/cib.1.1.6238

Bell-Doyon P, Laroche J, Saltonstall K, Villarreal Aguilar JC (2020) Specialized bacteriome uncovered in the coralloid roots of the epiphytic gymnosperm, *Zamia pseudoparasitica*. Environmental DNA:1–11. https://doi.org/10.1002/edn3.66

Brookes PC, Powlson DS, Jenkinson DS (1982) Measurement of microbial biomass phosphorus in soil. Soil Biol Biochem 14:319–329. https://doi.org/10.1016/0038-0717(82)90001-3

Callahan B, McMurdie P, Rosen M et al (2016a) DADA2: high-resolution sample inference from Illumina amplicon data. Nat Methods 13:581–583. https://doi.org/10.1038/nmeth.3869

Callahan B, Sankaran K, Fukuyama J et al (2016b) Bioconductor workflow for microbiome data analysis: from raw reads to community analyses [version 1; referees: 3 approved]. F1000Research 5:1–49. https://doi.org/10.12688/F1000RESEARCH.8986.1

Callahan B, Sankaran K, Julia A, McMurdie P, Holmes S (2017) Workflow for microbiome data analysis: from raw reads to community analyses. IOP Publishing. https://bioconductor.org/help/course-materials/2017/BioC2017/Day1/Workshops/Microbiome/MicrobiomeWorkflowII.html#acknowledgments. Accessed 20 May 2019

Cernava T, Erlacher A, Aschenbrenner IA, Krug L, Lassek C, Riedel K, Grube M, Berg G (2017) Deciphering functional diversification within the lichen microbiota by meta-omics. Microbiome 5:82. https://doi.org/10.1186/s40168-017-0303-5

Costa J-L, Paulsrud P, Rikkinen J, Lindblad P (2001) Genetic diversity of *Nostoc* Symbionts Endophytically associated with two bryophyte species. Appl Environ Microbiol 67:4393–4396. https://doi.org/10.1128/AEM.67.9.4393-4396.2001

Costa JL, Paulsrud P, Lindblad P (2002) The cyanobacterial tRNALeu (UAA) intron: evolutionary patterns in a genetic marker. Mol Biol Evol 19:850–857. https://doi.org/10.1093/oxfordjournals.molbev.a004142

Costa JL, Romero EM, Lindblad P (2004) Sequence based data supports a single *Nostoc* strain in individual coralloid roots of cycads. FEMS Microbiol Ecol 49:481–487. https://doi.org/10.1016/j.femsec.2004.05.001

Darnajoux R, Constantin J, Miadlikowska J, Lutzoni F, Bellenger JP (2014) Is vanadium a biometal for boreal cyanolichens? New Phytol 202:765–771. https://doi.org/10.1111/nph.12777

DeLuca T, Zackrisson O, Nilsson M, Sellstedt A (2002) Quantifying nitrogen-fixation in feather moss carpets of boreal forests. Nature 419:917–920. https://doi.org/10.1038/nature01051

DeLuca T, Zackrisson O, Gentili F et al (2007) Ecosystem controls on nitrogen fixation in boreal feather moss communities. Oecologia 152:121–130. https://doi.org/10.1007/s00442-006-0626-6

Desiró A, Duckett JG, Pressel S Villarreal JC, Bidartondo MI (2013) Fungal symbioses in hornworts: a chequered history. Proc R Soc B-Biol Sci 280:20130207. https://doi.org/10.1098/Rspb.2013.0207

Dixon P (2003) Computer program review VEGAN , a package of R functions for community ecology. J Veg Sci 14:927–930

Fedrowitz K, Kaasalainen U, Rikkinen J (2011) Genotype variability of *Nostoc* symbionts associated with three epiphytic Nephroma species in a boreal forest landscape. Bryologist 114:220–230. https://doi.org/10.1639/0007-2745-114.1.220

Gentili F, Nilsson M, Zackrisson O et al (2005) Physiological and molecular diversity of feather moss associative N 2-fixing cyanobacteria. J Exp Bot 56:3121–3127. https://doi.org/10.1093/jxb/eri309

Gotelli NJ, Colwell RK (2001) Quantifying biodiversity: procedures and pitfalls in the measurement and comparison of species richness. Ecol Lett 4:379–391. https://doi.org/10.1046/j.1461-0248.2001.00230.x

Gutiérrez-García K, Bustos-Dıaz ED, Corona-Gomez JA et al (2019) Cycad coralloid roots contain bacterial communities including cyanobacteria and *Caulobacter* spp. that encode niche-specific biosynthetic gene clusters. Genome Biol Evol 11:319–334. https://doi.org/10.1093/gbe/evy266

Holland-Moritz H, Stuart J, Lewis LR, Miller S, Mack MC, McDaniel SF, Fierer N (2018) Novel bacterial lineages associated with boreal moss species. Environ Microbiol 20:2625–2638. https://doi.org/10.1111/1462-2920.14288

Hughes JB, Hellmann JJ, Ricketts TH, Bohannan BJM (2001) Counting the uncountable: statistical approaches to estimating microbial diversity. Appl Environ Microbiol 10:4399–4406. https://doi.org/10.1128/AEM.67.10.4399

Joneson S, O'Brien H (2017) A molecular investigation of free-living and lichenized *Nostoc* sp. and symbiotic lifestyle determination. Bryologist 120:371–381. https://doi.org/10.1639/0007-2745-120.4.371

Klindworth A, Pruesse E, Schweer T, Peplies J, Quast C, Horn M, Glöckner FO (2013) Evaluation of general 16S ribosomal RNA gene PCR primers for classical and next-generation sequencing-based diversity studies. Nucleic Acids Res 41:1–11. https://doi.org/10.1093/nar/gks808

Knack JJ, Wilcox LW, Delaux P-M, Ané JM, Piotrowski MJ, Cook ME, Graham JM, Graham LE (2015) Microbiomes of Streptophyte algae and bryophytes suggest that a functional suite of microbiota fostered plant colonization of land. Int J Plant Sci 176:405–420. https://doi.org/10.1086/681161

Lavoie C, Renaudin M, Troy McMullin R, Gagnon J, Roy C, Beaulieu M-E, Bellenger JP, Villarreal JC (2020) Extremely low genetic diversity of Stigonema associated with Stereocaulon in eastern Canada. Bryologist 123:188–203. https://doi.org/10.1639/0007-2745-123.2.188

LeBauer DS, Treseder KK (2008) Nitrogen limitation of net primary productivity in terrestrial ecosystems is globally distributed. Ecology 89:371–379. https://doi.org/10.1890/06-2057.1

Lindo Z, Nilsson MC, Gundale MJ (2013) Bryophyte-cyanobacteria associations as regulators of the northern latitude carbon balance in response to global change. Glob Chang Biol 19:2022–2035. https://doi.org/10.1111/gcb.12175

Lodge DJ, McDowell WH, McSwiney CP (1994) The importance of nutrient pulses in tropical forests. Trends Ecol Evol 9:384–387. https://doi.org/10.1016/0169-5347(94)90060-4

Magain N, Miadlikowska J, Goffinet B, Sérusiaux E, Lutzoni F (2016) Macroevolution of specificity in cyanolichens of the genus *Peltigera* section *Polydactylon* (Lecanoromycetes, Ascomycota). Syst Biol 66:74–99. https://doi.org/10.1093/sysbio/syw065

McMurdie PJ, Holmes S (2013) Phyloseq: an R package for reproducible interactive analysis and graphics of microbiome census data. PLoS One 8:e61217. https://doi.org/10.1371/journal.pone.0061217

Meeks JC (2007) Physiological adaptations in nitrogen-fixing Nostoc–plant symbiotic associations. In: Prokaryotic symbionts in plants. Springer-Verlag, Berlin Heidelberg, pp 181–205

Nelson J, Shaw AJ (2019) Exploring the natural microbiome of the model liverwort: fungal endophyte diversity in *Marchantia polymorpha* L. Symbiosis. 78:45–59. https://doi.org/10.1007/s13199-019-00597-4

Nelson JM, Hauser DA, Hinson R, Shaw AJ (2018) A novel experimental system using the liverwort *Marchantia polymorpha* and its fungal

endophytes reveals diverse and context-dependent effects. New Phytol 218:1217–1232. https://doi.org/10.1111/nph.15012

Nelson JM, Hauser DA, Gudiño JA, Guadalupe YA, Meeks JC, Salazar Allen N, Villarreal JC, Li FW (2019) Complete genomes of symbiotic cyanobacteria clarify the evolution of vanadium-Nitrogenase. Genome Biol Evol 11:1959–1964. https://doi.org/10.1093/gbe/evz137

O'Brien H, Miadlikowska J, Lutzoni F (2005) Assessing host specialization in symbiotic cyanobacteria associated with four closely related species of the lichen fungus *Peltigera*. Eur J Phycol 40:363–378. https://doi.org/10.1080/09670260500342647

O'Brien HE, Miadlikowska J, Lutzoni F (2013) Assessing population structure and host specialization in lichenized cyanobacteria. New Phytol 198:557–566. https://doi.org/10.1111/nph.12165

Oksanen J, Blanchet FG, Friendly M, et al (2019) Package 'vegan.' Community Ecology Package. R package version 2.5–6

Pardo-De la Hoz CJ, Magain N, Lutzoni F et al (2018) Contrasting symbiotic patterns in two closely related lineages of Trimembered lichens of the genus *Peltigera*. Front Microbiol 9:1–14. https://doi.org/10.3389/fmicb.2018.02770

R Core Team R (2017) R core team. R: A Language and Environment for Statistical Computing [Internet]

Remy W, Taylor T, Hass H, Kerp H (1994) Four hundred-million-year-old vesicular arbuscular mycorrhizae. Proc Natl Acad Sci U S A 91:11841–11843. https://doi.org/10.1073/pnas.91.25.11841

Renzaglia KS (1978) A comparative morphology and developmental anatomy of the Anthocerotophyta. J Hattori Bot Lab 44:31–90

Renzaglia KS, Schuette S, Duff J et al (2007) Bryophyte phylogeny: advancing the molecular and morphological frontiers. Bryologist 110:179–213. https://doi.org/10.1639/0007-2745(2007)110[179:BPATMA]2.0.CO;2

Rikkinen J, Virtanen V (2008) Genetic diversity in cyanobacterial symbionts of thalloid bryophytes. J Exp Bot 59:1013–1021. https://doi.org/10.1093/jxb/ern003

Rousk K, Jones DL, DeLuca TH (2013) Moss-cyanobacteria associations as biogenic sources of nitrogen in boreal forest ecosystems. Front Microbiol 4:1–10. https://doi.org/10.3389/fmicb.2013.00150

RStudio Team (2015) RStudio: Integrated Development for R. RStudio, Inc., Boston, MA. http://www.rstudio.com/

Rudi K, Skulberg O, Jakobsen K (1998) Evolution of cyanobacteria by exchange of genetic material among Phyletically related strains. J Bacteriol 180:3453–3461. https://doi.org/10.1128/JB.180.13.3453-3461.1998

Schirrmeister B, de Vos J, Antonelli A, Bagheri H (2013) Evolution of multicellularity coincided with increased diversification of cyanobacteria and the great oxidation event. PNAS 110:1791–1796. https://doi.org/10.1073/pnas.1209927110

Schlesinger W, Klein EM, Vengosh A (2017) Global biogeochemical cycle of vanadium. Proc Natl Acad Sci U S A 114:E11092–E11100. https://doi.org/10.1073/pnas.1715500114

Sierra MA, Danko DC, Sandoval TA, Pishchany G, Moncada B, Kolter R, Mason CE, Zambrano MM (2020) The microbiomes of seven lichen genera reveal host specificity, a reduced Core Community and potential as source of antimicrobials. Front Microbiol 11:1–12. https://doi.org/10.3389/fmicb.2020.00398

Stamatakis A (2014) RAxML version 8: a tool for phylogenetic analysis and post-analysis of large phylogenies. Bioinformatics 30:1312–1313

Villarreal AJC, Renzaglia KS (2006) Structure and development of *Nostoc* strands in *Leiosporoceros dussi*i (Anthocerotophyta): a novel symbiosis in land plants. Am J Bot 93:693–705. https://doi.org/10.3732/ajb.93.5.693

Vincent AT, Derome N, Boyle B, Culley AI, Charette SJ (2017) Next-generation sequencing (NGS) in the microbiological world: how to make the most of your money. J Microbiol Methods 138:60–71. https://doi.org/10.1016/j.mimet.2016.02.016

Ward LM, Cardona T, Holland-Moritz H (2019) Evolutionary implications of Anoxygenic Phototrophy in the bacterial phylum Candidatus Eremiobacterota (WPS-2). Front Microbiol 10:1–19. https://doi.org/10.3389/fmicb.2019.01658

West NJ, Adams DG (1997) Phenotypic and genotypic comparison of symbiotic and free-living cyanobacteria from a single field site. Appl Environ Microbiol 63:4479–4484

Wickham H, Chang W (2009) ggplot2: an implementation of the grammar of graphics. R package version 0.8. 3

Wong FCY, Meeks JC (2002) Establishment of a functional symbiosis between the cyanobacterium *Nostoc punctiforme* and the bryophyte *Anthoceros punctatus* requires genes involved in nitrogen control and initiation of heterocyst differentiation the GenBank accession numbers for the cod. Microbiology 148:315–323. https://doi.org/10.1099/00221287-148-1-315

Wright D, Prickett T, Helm R, Potts M (2001) Form species *Nostoc commune* (cyanobacteria). Int J Syst Evol Microbiol 51:1839–1852. https://doi.org/10.1099/00207713-51-5-1839

Zheng Y, Chiang T-Y, Huang C-L, Gong X (2018) Highly diverse endophytes in roots of Cycas bifida (Cycadaceae), an ancient but endangered gymnosperm. J Microbiol 56:337–345. https://doi.org/10.1007/s12275-018-7438-3